SO_2-assisted simultaneous reduction of SO_2 and NO by CO on SnO_2–TiO_2 solid solution

Zhao-Qiong Liu, Jun Ma, Zhao-Liang Zhang, and Xi-Yao Yang *

College of Chemistry and Molecular Engineering, Peking University, Beijing 100871, P.R. China

Received 24 May 2002; accepted 20 November 2002

$Sn_{0.5}Ti_{0.5}O_2$ shows excellent catalytic performance both for the CO–SO_2 reaction and the CO–SO_2–NO reaction. At 350 °C, 525 ppm SO_2/520 ppm NO/2085 ppm CO, SV = 3000 h^{-1}, the conversion of SO_2 is nearly complete in the CO–SO_2 reaction and above 89% in the CO–SO_2–NO reaction; NO conversion is above 98% in the latter reaction. The selectivities of S and N_2 are both close to 100%. SO_2 shows a significant promoting effect on the activity of the $Sn_{0.5}Ti_{0.5}O_2$ catalyst for NO reduction by CO. Combining transient response experiments, catalytic tests and TPD results, we propose a SO_2-assisted NO–CO reaction concept. The existence of a surface sulfur species, which was formed during the CO–SO_2 or CO–SO_2–NO reaction, is proved by XPS analysis. It is the active site for NO reduction in the CO–SO_2–NO reaction, and through which SO_2 accomplishes its promoter role. On the basis of the results obtained, the SO_2-assisted redox mechanism of simultaneous reduction of SO_2 and NO by CO is proposed.

KEY WORDS: SnO_2–TiO_2; surface-active sulfur; reduction; NO; SO_2.

1. Introduction

SO_2 and NO as the two major air pollutants, which are usually emitted from coal- and oil-fired power plants, transportation, and domestic activities, and in many occasions simultaneously, are always the central issues in the environmental protection field. Much work has been carried out on separate catalytic reductions of NO to N_2 and SO_2 to S, in which CO as a reductant has attracted much attention owing to the simultaneous removal of both SO_2 (NO) and CO [1–4]. For the simultaneous removal of SO_2 and NO, wet lime/limestone scrubbers for desulfurization and selective catalytic reduction of NO with NH_3 have been commercialized [5], but the combination processes are complicated and produce a large amount of solid/liquid wastes that require further disposal. So, the dry-type sorbent/catalyst process for simultaneous removal of SO_2 and NO was developed [6–8], but in these processes SO_2 is oxidized to SO_3 and fixed on the catalysts as sulfates, which must be periodically removed for regeneration. In this regard, direct catalytic reduction of SO_2 and NO to elemental S and N_2 by CO in a one-way process has attracted much attention and has been under development [9–11]. However, in these systems a substantial amount of undesirable and toxic COS was formed and two-bed systems must be used to suppress the COS, which makes the process costly [10]. Recently, Ma *et al.* [12] reported that $La_2O_2S + CoS_2$ could be used as a catalyst for simultaneous reduction of SO_2 and NO by CO. $La_2O_2S + CoS_2$ as a SO_2–CO reaction catalyst has been widely studied [4,13–16], and a COS intermediate mechanism modified using the remote control concept has been proposed. When the catalyst was used for the SO_2–NO–CO reaction, based on the NO–COS reaction, it was believed that COS was also an intermediate. However, a detailed report has not yet been published. Zhuang *et al.* [17] reported a CoMo/Al_2O_3 catalyst for the SO_2–NO–CO reaction and suggested that the high catalytic activity of the sulfided catalyst originated from the moderate CoMo–S bond strength, which made it easy to form the intermediate COS and to regenerate the lattice sulfur. They also proposed the COS intermediate mechanism.

Our research group has found that a SnO_2–TiO_2 solid solution shows high catalytic activity for the simultaneous reduction of SO_2 and NO by CO (SRSN [18]), and there is no COS formation during the reaction. In the present work we report the catalytic performance of the $Sn_{0.5}Ti_{0.5}O_2$ catalyst for the SRSN reaction, and using the transient response method, TPD, XPS and XRD study the function of SO_2 in the NO–CO reaction, the active site and the mechanism of the SRSN reaction.

2. Experimental

2.1. Catalyst preparation

The $Sn_{0.5}Ti_{0.5}O_2$ solid solution catalyst was prepared by the coprecipitation method. The mixed solution of an equivalent mole of $Ti(SO_4)_2$ and $SnCl_4 \cdot 5H_2O$ and ammonia were simultaneously placed into deionized

* To whom correspondence should be addressed.
E-mail: yangxy@.pku.edu.cn

1011-372X/03/0300-0087/0

water under vigorous agitation, keeping the pH of the solution at 7–8 during the precipitation process. The solution was then aged for 1 h. The resultant precipitate was washed until free from Cl^- and SO_4^{2-} and then dried at 120 °C for 15 h and calcined at 500 °C for 5 h in air. Its BET surface area was 95 m^2/g measured using a Micromeritics ASAP 2010.

2.2. Catalyst characterization

2.2.1. XRD measurement

Powder X-ray diffraction (XRD) analyses were performed to probe for the kinds of crystal phases present in the catalysts that experienced different reactions. The XRD patterns were obtained using a Rigaku D/max2000 Auto X-ray diffractometer with CuKα radiation ($\lambda = 1.5415$ Å) and Ni filter 0.4 incoming slit.

2.2.2. XPS analysis

X-ray photoelectron spectroscopy (XPS) was used to determine the surface sulfur-containing species. It was conducted using a VG ESCALAB55 X-ray photoelectron spectrometer with a monochromatic AlKα source (1486.6 eV).

2.3. Catalyst performance and surface reactivity studies

The flow system used for performing catalytic testing and various kinds of transient experiments is shown in figure 1. Mass-flow control (MFC) valves were used to prepare *in situ* a given gas mixture. Good mixing of the gas streams was achieved through the mixing chamber. The six-way valve was used to convert the streams that go through the catalyst. The studied stream via a six-way valve bypasses the reactor to the quadrupole mass spectrometer (QMS) until all the signals become stable, which describes the base relative concentration of the initial feed gas. Then the stream was switched to the reactor, the signal change described the concentration change of the reactants and products and the four-way valve resulted in the gas stream being detected by the QMS. The QMS (LZL-204, Beijing Analytical Instrument Plant) was equipped with a fast response inlet capillary/leak diaphragm system, and the vacuum was better than 10^{-5} Pa.

For MS analyses, mass numbers (m/z) used were 28, 30, 32, 44, 60 and 64 for CO (or N_2), NO, O_2, CO_2 (or N_2O), COS and SO_2, respectively. Gaseous responses were calibrated every day using standard gas mixtures. For gases of N_2O, CO, COS and SO_2, an on-line FTIR spectrometer (vector 22, Bruker) was also used to calibrate the exit concentrations.

The microreactor used in the present work was a U-type glass tube (17 cm long and a 3 mm i.d.). A frit layer was put at the effluent side of the reactor to capture the produced sulfur. A small furnace controlled by a programmable temperature controller provided the heat for the reactor. The temperature of the catalyst was measured by a "K"-type thermocouple placed in the middle of the catalyst bed.

For a catalytic measurement, 0.3 g of catalyst (40–60 meshes) was loaded into the reactor. The feed stream was provided by 2100 ppm SO_2/Ar, 2080 ppm NO/Ar and 4160 ppm CO/Ar. Controlled by the MFC valves, the required feed gas was obtained. GHSV was 3000 h^{-1}.

The standard pretreatment of a fresh sample was a 2 h initial calcination in flowing HP argon at 500 °C followed by cooling of the sample to the appropriate temperature for the subsequent experiment.

Conversion and selectivity of SO_2 and NO in a steady reaction were defined as follows:

SO_2:

$$\text{Conversion } (\%) = \frac{(SO_2)_{inlet} - (SO_2)_{outlet}}{(SO_2)_{inlet}} \times 100$$

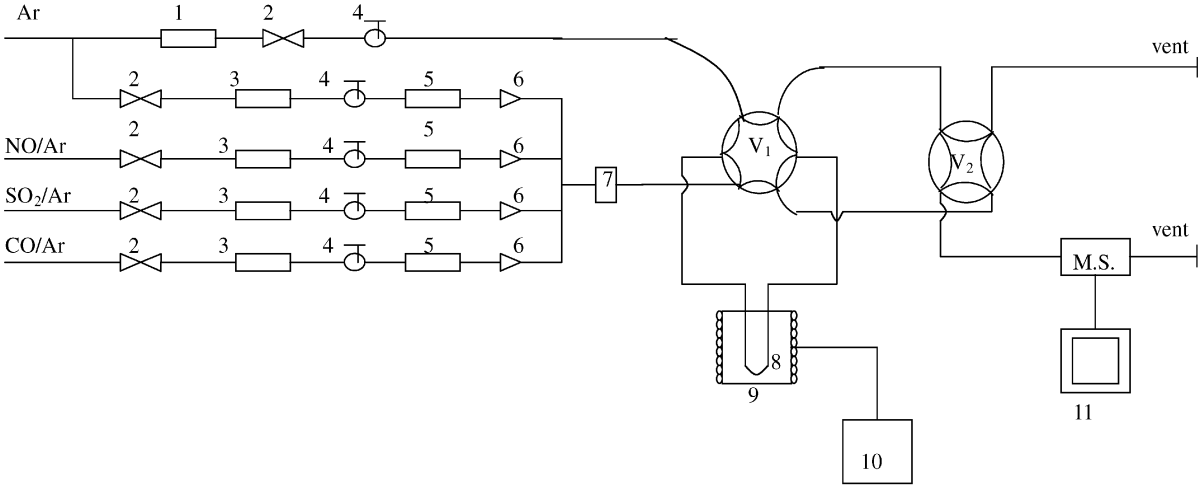

Figure 1. Flow system for catalytic tests: 1, water and oxy-traps; 2, on/off valves; 3, filter; 4, pressure regulator; 5, mass flow control valve; 6, one-way valve; 7, mixing chamber; 8, reactor; 9, furnace; 10, temperature controller; 11, computer (MS, mass spectrometer; V_1, six-way valve; V_2, four-way valve).

S:

$$\text{Selectivity (\%)} = \frac{(SO_2)_{inlet} - (SO_2)_{outlet} - (COS)_{outlet}}{(SO_2)_{inlet} - (SO_2)_{outlet}} \times 100$$

NO:

$$\text{Conversion (\%)} = \frac{(NO)_{inlet} - (NO)_{outlet}}{(NO)_{inlet}} \times 100$$

N2:

$$\text{Selectivity (\%)} = \frac{(NO)_{inlet} - (NO)_{outlet} - (N_2O)_{outlet}}{(NO)_{inlet} - (NO)_{outlet}} \times 100$$

where (SO_2), (COS), (NO) and (N_2O) represent the intensity on MS (or FTIR) of the corresponding materials.

2.4. Transient response experiments

A series of transient response experiments was carried out to understand the detailed information of the reactions. The detailed response steps will be described in the text later.

2.5. TPD experiments

Temperature-programmed desorption (TPD) experiments were performed on the same reactor to examine the character of surface sulfur species on the catalysts after reactions and adsorption processes. An amount of 0.2 g of $Sn_{0.5}Ti_{0.5}O_2$ catalyst was loaded in the reactor and was pretreated *in situ* in an Ar stream (30 ml/min) at 500 °C for 1 h, and then cooled to 350 °C. After that we carried out the following operations: (a) SO_2–CO reaction for 2 h; (b) SO_2 adsorption to equilibrium; (c) CO reaction to equilibrium then purged with Ar for 1 h and then SO_2 adsorption, the stream was changed to Ar and cooled to room temperature. Finally, TPD experiments were carried out in Ar at 20 ml/min at a heating rate of 10 °C/min from 25 to 500 °C. During the TPD, effluent SO_2 was recorded by the QMS on line.

3. Results

3.1. Catalyst characterization

3.1.1. X-ray diffraction studies

XRD patterns of the catalysts before and after different reactions are shown in figure 2. It can be seen that the crystal structure of the fresh catalyst is a typical rutile. In general, anatase is obtained when TiO_2 was calcined at 500 °C [19], while SnO_2 is a typical rutile. This indicates that the interaction between SnO_2 and TiO_2 has taken place so that Ti cations were incorporated into the lattice of rutile SnO_2 and formed a homogeneous solid solution. That resulted in the transformation of TiO_2 from anatase to rutile occurring at a lower temperature. Catalysts that have undergone the $CO + SO_2$ reaction and the $CO + SO_2 + NO$ reaction have the same XRD patterns as the fresh catalyst. This indicates that there is neither structure change during these reactions nor new phase formation after the reactions. Nevertheless, the catalyst that underwent sulfurization by $H_2S + H_2$ mainly existed as SnS.

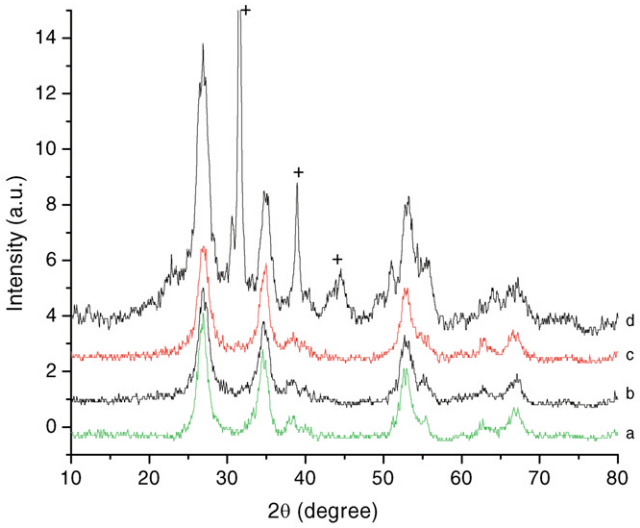

Figure 2. XRD patterns of catalysts before and after different reactions: (a) before reaction; (b) after CO–SO_2 reaction; (c) after CO–SO_2–NO reaction; (d) after $H_2S + H_2$ reaction.

3.1.2. XPS

Figure 3 shows the weak peak of S_{2P} tested by XPS, which indicates that a sulfur species was formed on the surface of the catalyst. However, for the fresh sample

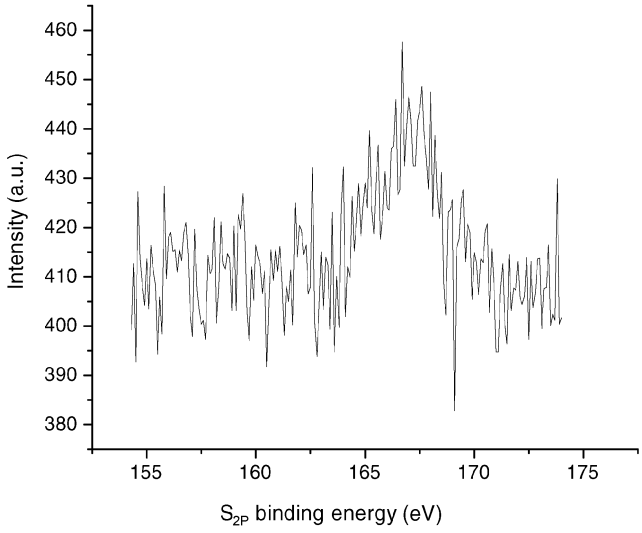

Figure 3. XPS spectrum of the $Sn_{0.5}Ti_{0.5}O_2$ catalyst after CO–SO_2 reaction.

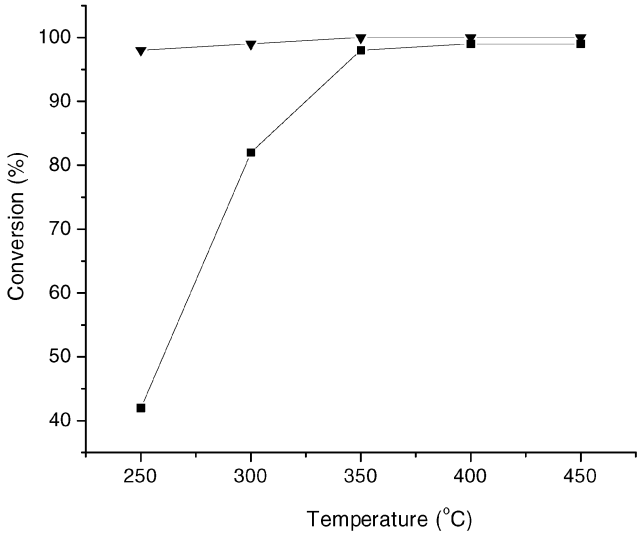

Figure 4. Conversion of SO_2 and the selectivity towards elemental sulfur as a function of temperature over $Sn_{0.5}Ti_{0.5}O_2$ catalyst. Feed gas: SO_2, 1050 ppm; CO, 2085 ppm, Ar, SV = 3000 h^{-1}. (■) SO_2 conversion; (▼) S selectivity.

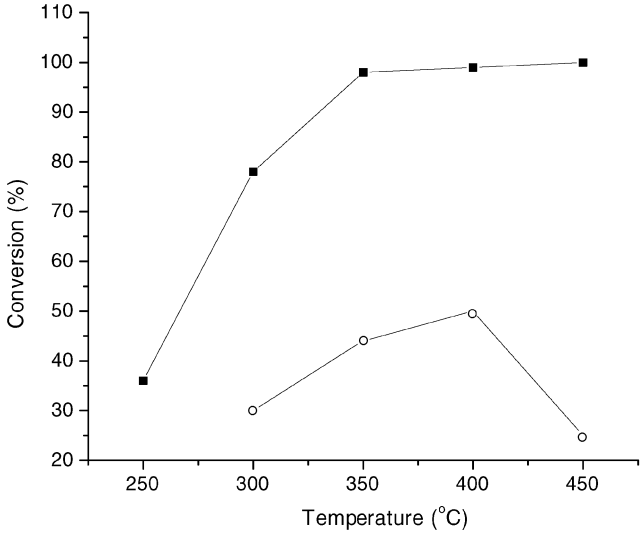

Figure 5. Conversion of NO to N_2 of the reaction NO + CO as a function of temperature over $Sn_{0.5}Ti_{0.5}O_2$ catalyst before and after CO–SO_2 reaction. Feed gas: NO, 520 ppm; CO, 1040 ppm, Ar, SV = 3000 h^{-1}. (○) Before CO–SO_2 reaction; (■) after CO–SO_2 reaction.

there was no sulfur species detected. This confirms that the sulfur species does not originate from the material used in the catalyst preparation but from the reaction. The peak at 166.7 eV is attributed to SO_3^{2-}.

3.2. Catalytic performance

3.2.1. CO–SO_2 reaction

Figure 4 shows the conversion of SO_2 and the selectivity toward elemental sulfur as a function of reaction temperature over $Sn_{0.5}Ti_{0.5}O_2$. At temperatures higher than 350 °C, almost complete conversion of SO_2 with 100% selectivity was achieved.

Woo *et al.* [20] reported a mechanical mixture of SnO_2 and TiO_2 used for SO_2 reduction by CO. They obtained a 90% conversion and selectivity at 350 °C. After reaction, SnO_2 changed to SnS_2 and SnS. They proposed a redox mechanism based on the COS intermediate and bifunctionality concept. In the present work, the $Sn_{0.5}Ti_{0.5}O_2$ catalyst prepared by the coprecipitation method not only had a higher catalytic activity and selectivity, but there was no catalyst phase change (i.e., oxide does not change to sulfide) according to XRD. Also there was no COS formation detected during the reaction. At the effluent side of the reactor there was sulfur trapped on the frit.

3.2.2. NO–CO reaction

The fresh catalyst shows low activity for the NO–CO reaction. The maximum conversion is only 50% (figure 5).

3.2.3. NO–CO reaction after CO–SO_2 reaction

After experiencing the CO–SO_2 reaction at 350 °C, the catalyst shows a very high NO reduction activity (figure 5). At temperatures above 350 °C, a nearly 100% conversion of NO was achieved. From the XPS and XRD analysis, we know that after the CO–SO_2 reaction there was no noticeable change in the catalyst structure except the existence of surface sulfur species. So, it is suggested that the remarkably improved catalytic performance for the CO–NO reaction could only result from the surface sulfur species.

3.2.4. NO–CO–SO_2 reaction

The catalytic performance of simultaneous reduction of SO_2 and NO by CO on the $Sn_{0.5}Ti_{0.5}O_2$ catalyst is shown in figure 6. Compared to the separated CO–NO

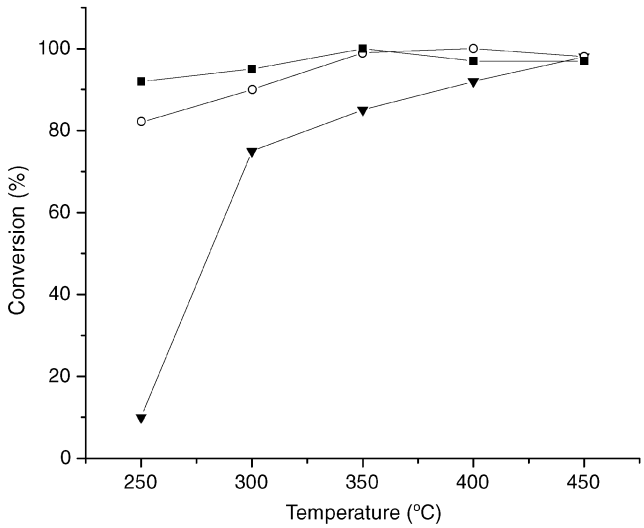

Figure 6. NO–CO–SO_2 reaction over $Sn_{0.5}Ti_{0.5}O_2$ catalyst. Feed gas: SO_2, 525 ppm; NO, 520 ppm; CO, 2085 ppm, Ar, SV = 3000 h^{-1}. (▼) SO_2 conversion; (○) NO conversion; (■) S selectivity.

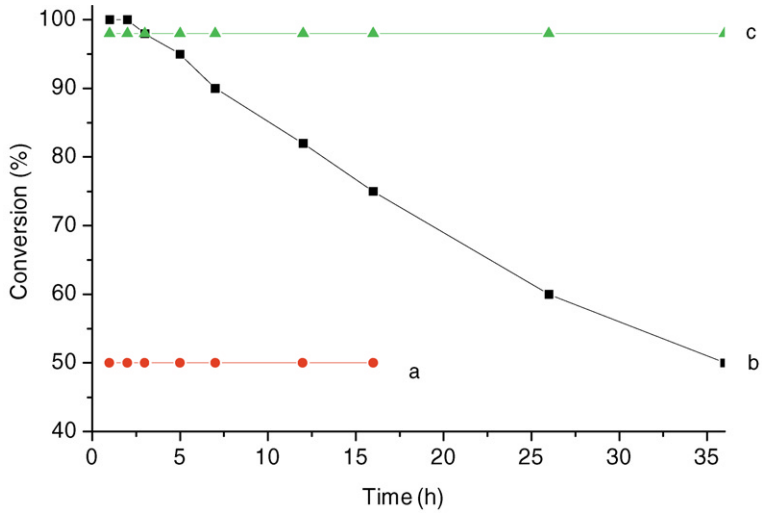

Figure 7. Reaction stability of NO conversion: (a) NO reduction by CO on the fresh catalyst; (b) NO reduction by CO after CO–SO_2 reaction; (c) SO_2–NO–CO reaction on the fresh catalyst.

reaction, it is evident that because SO_2 was added to the gas feed, the NO conversion was improved greatly. This indicates that SO_2 has a promoting effect on the activity of the $Sn_{0.5}Ti_{0.5}O_2$ catalyst for NO reduction with CO. On the contrary, the activity of SO_2 reduction is restrained compared to the SO_2–CO reaction without NO. This phenomenon will be discussed in another article.

3.3. *Stability of catalysts for different reactions*

The stability of catalysts for NO + CO, NO + CO (after SO_2–CO reaction) and SO_2 + NO + CO at 400 °C is shown in figure 7. For NO reduction by CO on the fresh catalyst, a low but stable catalytic activity is shown (figure 7(a)). After the CO–SO_2 reaction the catalyst shows a high initial NO decomposition activity but deactivates finally (figure 7(b)). For the simultaneous reduction of SO_2 and NO by CO, the fresh catalyst shows not only a high NO conversion but also a high stability (figure 7(c)). During the 36 h test, there was no deactivation observed.

3.4. *Transient experiments*

The detailed response steps are described in table 1. Take experiment A as an example. Before the NO/Ar transient experiment, the catalyst was pretreated in a SO_2 + CO stream at 350 °C for 2 h and then purged with Ar for 60 min. Figure 8 shows the transient response curves after the feed gas changed to NO on a catalyst that had experienced the SO_2–CO reaction. The NO response curve decreases immediately at the change and then rises slowly. In the meantime, N_2O appears and when it reaches its maximum, N_2 starts to form accompanied by emission of SO_2. The shapes of the N_2 and SO_2 responses are highly correlated, implying that N_2 and SO_2 production takes place simultaneously. Note that no O_2 is detected. The facts given above indicate a nearly complete initial conversion of NO, which occurred as a reduction reaction on the active sulfur species. The NO reduction follows the formation of N_2O as the intermediate, and the produced "O" of NO combines with the active sulfur species to generate SO_2. A more detailed explanation will be provided later.

Here, the reaction of NO takes place on the catalyst after the CO + SO_2 reaction. There are oxygen vacancies on the catalyst surface. We believe that the reaction of NO is a kind of reduction.

If the feed gas is changed to NO + CO (figure 9), the NO response curve also shows an immediate decrease but does not rise like that in figure 8. CO was oxidized and CO_2 was produced at the same time, and SO_2 appears 2 min later after the feed gas change. The amount of N_2O

Table 1
Description of sequential step changes of gas flow during transient response experiments

Experiment	Sequence of step changes of gas flow over the catalyst sample
A	SO_2 + CO reaction (350 °C, 2 h) → Ar (60 min, 350 °C)) → NO/Ar (350 °C)
B	SO_2 + CO reaction (350 °C, 2 h)) → Ar (60 min, 350 °C)) → NO/Ar + CO/Ar (350 °C)
C	SO_2 + CO reaction (350 °C, 2 h)) → Ar (60 min, 350 °C)) → CO/Ar (350 °C)
D	Ar (500 °C, 1 h)) → NO + CO + SO_2 (350 °C)

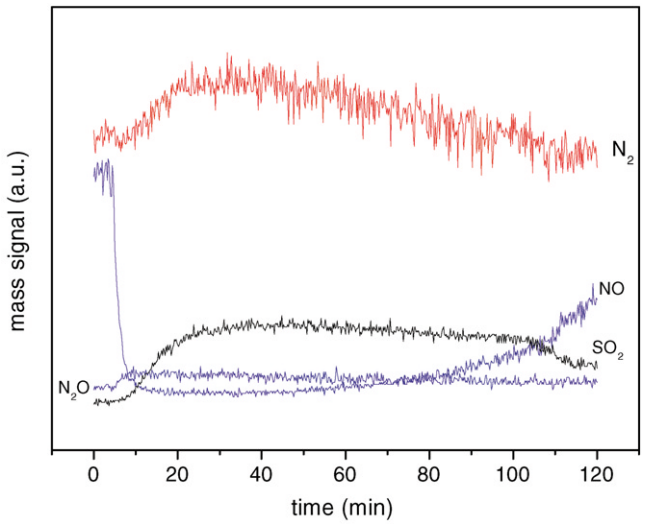

Figure 8. Transient response of NO stream on the catalyst after SO_2–CO reaction (detailed description in table 1).

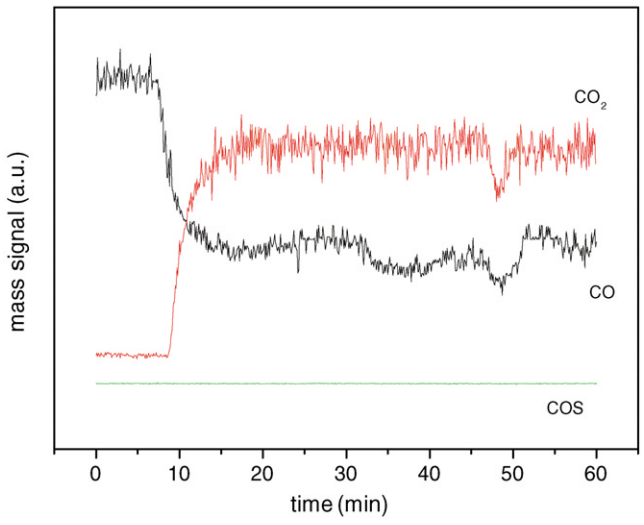

Figure 10. Transient response of the CO stream on the catalyst after the SO_2–CO reaction (detailed description in table 1).

was small as compared with CO_2 (by FTIR), so the signal of 44 mainly reflects the concentration change of CO_2. Some 20 min later the reaction reaches its balance and gives a NO conversion close to 100%.

On the catalyst after the CO–SO_2 reaction, CO can still be oxidized to CO_2 (figure 10), indicating that the catalyst surface was still in an oxide state. There is no COS observed. This result differs from previous conclusions [4,9,11,21], that is, CO reacts easily with adsorbed sulfur or crystal sulfur to form COS. In those reaction mechanisms COS is an important intermediate. For the present studied catalyst, as will be discussed later, surface "sulfur" combines with oxygen to produce SO_2 and does not combine with CO to produce COS. This is the important character of the $Sn_{0.5}Ti_{0.5}O_2$ catalyst.

Simultaneous reduction of SO_2 and NO by CO on the fresh catalyst was also examined by the transient response method (figure 11). CO and SO_2 both decrease quickly, and NO reaches balance slowly. The shape of the CO_2 curve is an overshoot. Kobayashi [22] studied the relationship of the reaction mechanisms and the transient response curves using a digital computer simulation. The overshoot response was owing to slow regeneration of active site or competitive adsorption of reactants. In this work, SO_2 is more easily adsorbed than CO and NO. The quick adsorption of SO_2 may occupy the active site of CO oxidation. This phenomenon also indicates that the regeneration of active sites for CO_2 formation is a rate-controlling step.

3.5. *TPD experiments*

Figure 12 shows the TPD profiles of SO_2 on different catalysts. The amount of SO_2 desorbed on the fresh

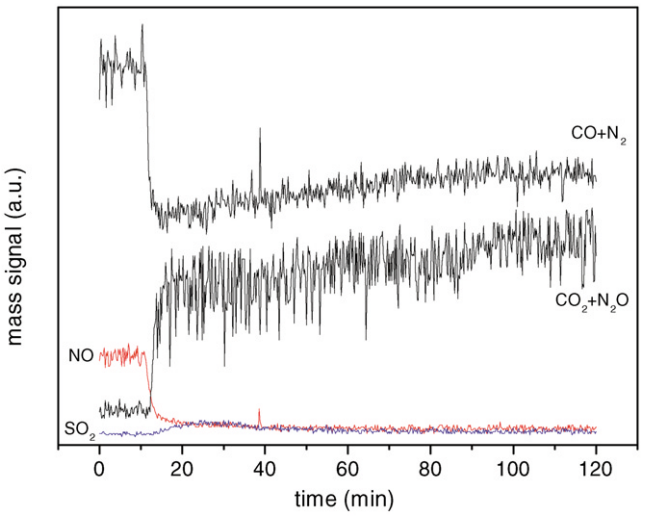

Figure 9. Transient response of NO–CO stream on the catalyst after SO_2–CO reaction (detailed description in table 1).

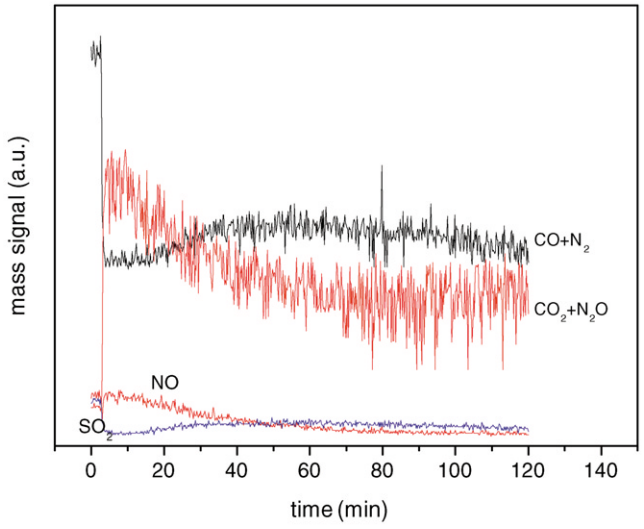

Figure 11. Transient response of the NO–CO–SO_2 stream on the fresh catalyst (detailed description in table 1).

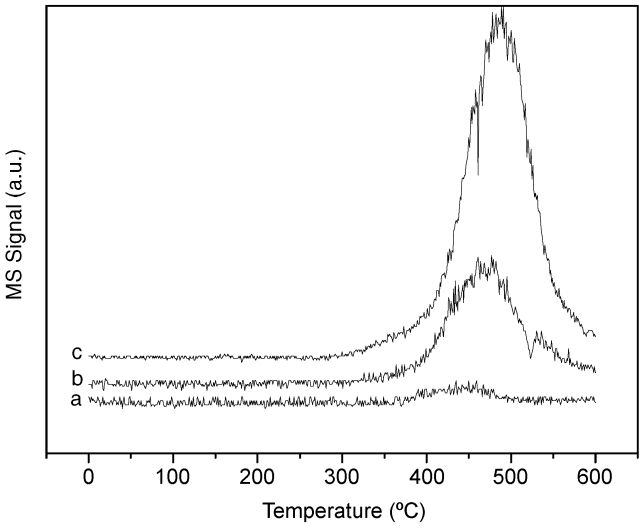

Figure 12. TPD profiles of SO_2 on different catalysts: (a) on the fresh catalyst; (b) on the reduced catalyst; (c) after the CO–SO_2 reaction.

catalyst is small (figure 12(a)). This kind of SO_2 should be pure desorption, because SO_2 does not react with the fresh catalyst under the experimental conditions.

It is obvious that the amount of SO_2 desorbed is greater (figure 12(b)) for the CO pre-reduced catalyst. Hence there should be other sulfur species, or SO_2 can adsorb more on the pre-reduced catalyst.

After the CO–SO_2 reaction, the amount of desorbed SO_2 was even more than that for the pre-reduced catalyst (figure 12(c)). Previous research suggested that after the CO–SO_2 reaction a surface sulfur species was formed. In the present work, under the reduced atmosphere, it is easier for the surface sulfur species to stay on the catalyst and form an adsorbed surface sulfur species. On heating, it may react with surface lattice O and desorb as SO_2.

4. Discussion

4.1. The active species to promote the NO–CO reaction

From the results of the catalytic tests, we noticed that after the CO–SO_2 reaction the catalytic performance of $Sn_{0.5}Ti_{0.5}O_2$ for the NO–CO reaction was greatly improved. XPS analysis proved the existence of sulfur species on the catalyst surface. Therefore it is suggested that the surface sulfur species are the active species for the NO–CO reaction. But what are the sulfur species?

After the CO–SO_2 reaction, there perhaps form sulfides, adsorbed surface sulfur species or adsorbed SO_2 on the catalyst surface. XRD could not detect any sulfides. So, the active species could not be sulfides. As to the adsorbed SO_2, from the TPD results (figure 12) we can see that there is some SO_2 adsorbed on the catalyst, but according to our catalytic tests the adsorbed SO_2 cannot improve the CO–SO_2 reaction (not shown here). Furthermore, the amount of SO_2 desorbed is quite different. After the CO–SO_2 reaction there was much more SO_2 desorbed, hence, except the adsorbed SO_2, there should be adsorbed active sulfur species, which was produced by the CO–SO_2 reaction. At higher temperatures, the highly active surface sulfur species combines with lattice oxygen on the catalyst and produces SO_2. This is consistent with the transient response experiments (figure 8) in which SO_2 was produced during the NO decomposition reaction. So, we come to the conclusion that active surface sulfur species is the active species, which promotes the NO–CO reaction.

4.2. Mechanism of SO_2-assisted CO–NO reaction

Catalytic tests prove that SnO_2–TiO_2 shows high catalytic activity for the CO–SO_2 reaction and not for the CO–NO reaction. But when SO_2 and NO are both in the feed gas, that is, as a CO–SO_2–NO reaction, the catalyst shows excellent catalytic performance not only for SO_2 reduction but also for NO reduction. This indicates that for the SnO_2–TiO_2 catalyst SO_2 is a promoter for the NO–CO reaction. How SO_2 promotes the CO–NO reaction is an interesting theoretical problem.

For the catalytic reduction of SO_2 to sulfur by CO there are two mechanisms suggested in the literature. The first one is the redox mechanism [23–25]:

$$\mathrm{Cat[O]} + \mathrm{CO} \longrightarrow \mathrm{Cat[\,]} + \mathrm{CO_2} \quad (1)$$

$$\mathrm{Cat[\,]} + \mathrm{SO_2} \longrightarrow \mathrm{Cat[O]} + \mathrm{SO} \quad (2)$$

$$\mathrm{Cat[\,]} + \mathrm{SO} \longrightarrow \mathrm{Cat[O]} + \mathrm{S}. \quad (3)$$

The second mechanism is the COS intermediate mechanism on the sulfide catalyst [26,27]:

$$\mathrm{MS}_X + \mathrm{CO} \longrightarrow \mathrm{MS}_{X-1} + \mathrm{COS} \quad (4)$$

$$2\mathrm{COS} + \mathrm{SO_2} \longrightarrow 3/2\mathrm{S_2} + 2\mathrm{CO_2} \quad (5)$$

$$\mathrm{MS}_{X-1} + \mathrm{S} \longrightarrow \mathrm{MS}_X. \quad (6)$$

In the present work, we prefer the first typical redox mechanism. The CO-TPR experiments prove that CO could be oxidized by SnO_2–TiO_2 and produce CO_2 (not shown); on the other hand, over the SnO_2–TiO_2 catalyst, CO can react with SO_2 and produce CO_2 and sulfur. So the CO–SO_2 reaction is a typical redox reaction. It is more plausible according to the results of this work.

For the reduction of NO by CO on an iron oxide catalyst, it was suggested [28] that it is a typical redox reaction:

$$\mathrm{Cat[\,]} + \mathrm{NO} \longrightarrow \mathrm{Cat[O]} + \mathrm{N_2O} \quad (7)$$

$$\mathrm{Cat[\,]} + \mathrm{N_2O} \longrightarrow \mathrm{Cat[O]} + \mathrm{N_2}. \quad (8)$$

We believe that it is also a redox reaction on the SnO_2–TiO_2 catalyst and the oxygen ion vacancy is the active

site for this reaction. However, when SO_2 is added to the feed gas, the dramatically improved catalytic performance of NO conversion cannot be explained by the simple redox mechanism.

After the CO–SO_2 reaction, the transient responses of the NO stream (figure 8) or the NO–CO stream (figure 9) prove the quick response of NO, and the formation of SO_2 is a little retarded. As time goes on, the NO conversion reaction gradually stops. Why is there SO_2 production in the transient response experiment and how is it formed?

From the discussion of the active species for the NO–CO reaction, we know that surface sulfur species as the active species is very active; it can combine with oxygen to produce SO_2 on heating. We speculate that when NO is adsorbed on the active site, the highly active surface sulfur activates the N–O bond and causes it to split into N_2O and O, and active sulfur combines with the produced O and forms SO_2; hence the oxygen on the catalyst surface is transferred in time and promotes the NO reduction. Once the surface active sulfur is used up, the decomposition reaction will cease:

$$\mathrm{Cat[\,]} + \mathrm{S^*} \longrightarrow \mathrm{Cat[\,]S^*} \quad (9)$$

$$\mathrm{Cat[\,]S^*} + \mathrm{NO} \longrightarrow \mathrm{Cat[O]} + \mathrm{N_2O} + \mathrm{SO_2} \quad (10)$$

$$\mathrm{Cat[\,]S^*} + \mathrm{N_2O} \longrightarrow \mathrm{Cat[O]} + \mathrm{N_2} + \mathrm{SO_2} \quad (11)$$

where S^* represents surface sulfur species.

The catalytic stability experiments also confirm the important role of surface sulfur species. The NO reduction activity of the catalyst after the CO–SO_2 reaction is finally deactivated (figure 8(a)). This is because the amount of active sulfur species formed after the CO–SO_2 reaction is limited, so the catalyst is finally deactivated. However, when SO_2 and CO are added at the same time to the NO stream, reactions (1)–(3), (9) and (11) can recycle completely and active sulfur species can also be recovered completely. Therefore, the activity of the catalyst can be maintained (figure 7(c)).

According to the above discussion, we propose the following mechanism of SO_2-assisted simultaneous reduction of SO_2 and NO by CO:

$$\mathrm{Cat[O]} + \mathrm{CO} \longrightarrow \mathrm{Cat[\,]} + \mathrm{CO_2} \quad (1)$$

$$\mathrm{Cat[\,]} + \mathrm{SO_2} \longrightarrow \mathrm{Cat[O]} + \mathrm{SO} \quad (2)$$

$$\mathrm{Cat[\,]} + \mathrm{SO} \longrightarrow \mathrm{Cat[O]} + \mathrm{S} \quad (3)$$

$$\mathrm{Cat[\,]} + \mathrm{NO} \longrightarrow \mathrm{Cat[O]} + \mathrm{N_2O} \quad (7)$$

$$\mathrm{Cat[\,]} + \mathrm{N_2O} \longrightarrow \mathrm{Cat[O]} + \mathrm{N_2} \quad (8)$$

$$\mathrm{Cat[\,]} + \mathrm{S^*} \longrightarrow \mathrm{Cat[\,]S^*} \quad (9)$$

$$\mathrm{Cat[\,]S^*} + \mathrm{NO} \longrightarrow \mathrm{Cat[O]} + \mathrm{N_2O} + \mathrm{SO_2} \quad (10)$$

$$\mathrm{Cat[\,]S^*} + \mathrm{N_2O} \longrightarrow \mathrm{Cat[O]} + \mathrm{N_2} + \mathrm{SO_2}. \quad (11)$$

Obviously, for the SRSN reaction, there are two kinds of active centers on the SnO_2–TiO_2 catalyst, one is an oxygen ion vacancy, Cat[ ], and the other is surface-active sulfur, $\mathrm{Cat[\,]S^*}$. The nature of active surface sulfur is now under study.

5. Conclusions

SnO_2–TiO_2 solid solution is an excellent catalyst for SRSN, while SO_2 acts as promoter for the NO–CO reaction in SRSN. It is shown that the promotion effect of SO_2 proceeds through the redox process of surface-active sulfur species (SAS formed during SRSN); therefore, SAS with oxygen ion vacancy together constitute the active site for SRSN. On the basis of the above discovery, the concept of the SO_2-assisted NO–CO reaction and SO_2-assisted redox mechanism of SRSN is proposed.

Acknowledgments

The authors are grateful to Prof. Nianzu Wu for his help in finishing the XPS measurements, and for the financial support from the National Key Basis Research Program (G19990222) and National Science Foundation China (20077002).

References

[1] I. Spassova, M. Khristova, D. Panayotov and D. Mehandjiev, J. Catal. 185 (1999) 43.
[2] V.C. Belessi, T.V. Bakas, C.N. Costa, A.M. Efstathiou and P.J. Pomonis, Appl. Catal. B 18 (2000) 13.
[3] W. Li, A.F. Sarofim and M. Flytzani-Stephanopoulos, Appl. Catal. B 4 (1994) 167.
[4] J.X. Ma, M. Fang and N.T. Lau, Appl. Catal. A 150 (1997) 253.
[5] J. Blanco, A. Bahamonde, E. Alvarez and P. Avila, Catal. Today 42 (1998) 85.
[6] S. Kasaoka, E. Sasaoka and H. Iwasaki, Bull. Chem. Soc. Jpn. 62 (1989) 1226.
[7] S. Gao, N. Nakagawa, K. Kato, M. Inomata and F. Tsuchiya, Catal. Today 29 (1996) 165.
[8] S.M. Jeong and S.O. Kim. Ind. Chem. Eng. Res. 39 (2000) 1911.
[9] C.W. Quinlan, V.C. Okay and J. R. Kittrell, Ind. Eng. Chem. Process. Des. Develop. 12 (1973) 359.
[10] C.W. Quinan, V.C. Okay and J. R. Kittrell. Ind. Eng. Chem. Prod. Res. Dev. 12 (1973) 3.
[11] V.N. Goetz, A. Sood and J.R. Kittrell, Ind. Eng. Chem. Prod. Res. Dev. 13 (1974) 110.
[12] J.X. Ma, M. Fang and N.T. Lau. Catal. Lett. 62 (1999) 127.
[13] J.X. Ma, M. Fang and N.T. Lau, J. Catal. 158 (1996) 251.
[14] J.X. Ma, M. Fang and N.T. Lau, J. Catal. 163 (1996) 271.
[15] N.T. Lau and M. Fang, J. Catal. 179 (1998) 343.
[16] N.T. Lau. M. Fang and J.X. Ma, Appl. Catal. B 26 (2000) 81.
[17] S.X. Zhuang, M. Yamazaki and K. Omata, Appl. Catal. B 31 (2001) 133.
[18] Z.L. Zhang, J. Ma and X.Y. Yang, Acta Phys. Chim. Sin. 17 (2001) 481.
[19] S. Matsuda and A. Kato, Appl. Catal. 8 (1983) 149.
[20] H.C. Woo, J.W. Lee, H. Kim, J.S. Chung and D.W. Park, 15th Meeting of the North American Catalysis Society, Chicago, IL, 18–22 May 1997, p. 38.

[21] S.X. Zhuang, H. Magara and M. Yamazaki, Appl. Catal. B 24 (2000) 89.
[22] M. Kobayashi, Chem. Eng. Sci. 37 (1982) 393.
[23] W. Liu and M. Flytzani-Stephanopoulos, ACS Symp. Ser. 552 (1994) 375.
[24] J. Happel, A.L. Leon, M.A. Hntow and L. Bajars, Ind. Eng. Chem. Prod. Res. Dev. 16 (1977) 150.
[25] D.B. Hibbert and R.H. Cabell, Appl. Catal. 41 (1988) 289.
[26] J.A. Baglio, Ind. Eng. Chem. Prod. Res. Dev. 21 (1982) 38.
[27] L.A. Haas and S.E. Khalafalla, J. Catal. 29 (1973) 264.
[28] H. Randall, R. Doepper and A. Renken, Appl. Catal. B 17 (1998) 357.
[29] Y. Teraoka, H. Fukuda and S. Kaganwa, Chem. Lett. (1990) 1.